



Genetic and microscopic assessment of the human chemotherapy-exposed placenta reveals possible pathways contributive to fetal growth restriction

M. Verheecke ^{a, b}, A. Cortès Calabuig ^c, J. Finalet Ferreiro ^c, V. Brys ^c, R. Van Bree ^d, G. Verbist ^c, T. Everaert ^a, L. Leemans ^a, M.M. Gziri ^e, I. Boere ^f, M.J. Halaska ^g, J. Vanhoudt ^c, F. Amant ^{a, h, *}, K. Van Calsteren ^{b, d}

^a Department of Oncology, KU Leuven, Herestraat 49, 3000 Leuven, Belgium

^b Department of Obstetrics and Gynecology, University Hospitals Leuven, Herestraat 49, 3000 Leuven, Belgium

^c Genomics Core, KU Leuven, Herestraat 49, 3000 Leuven, Belgium

^d Department of Reproduction and Regeneration, KU Leuven, Herestraat 49, 3000 Leuven, Belgium

^e Department of Obstetrics and Gynecology, Cliniques Universitaires St. Luc, Hippocrateslaan 10, 1200 Brussels, Belgium

^f Department of Medical Oncology, Erasmus MC Cancer Institute, 's-Gravendijkwal 230, 3015 CE Rotterdam, The Netherlands

^g Department of Obstetrics and Gynaecology, 3rd Medical Faculty, Charles University, Prague 5, Faculty Hospital Kralovske Vinohrady, Srobarova 1150/50, 100 34, Prague 10, Czech Republic

^h Department of Gynaecologic Oncology, Center for Gynaecologic Oncology, Amsterdam, Plesmanlaan 121, 1066 CX, Amsterdam, The Netherlands

ARTICLE INFO

Article history:

Received 3 September 2017

Received in revised form

6 March 2018

Accepted 7 March 2018

Keywords:

Placenta

Fetal growth restriction

Chemotherapy

Oxidative damage

Proliferation

ABSTRACT

Introduction: Fetal growth restriction (FGR) carries an increased risk of perinatal mortality and morbidity. A major cause of FGR is placental insufficiency. After in utero chemotherapy-exposure, an increased incidence of FGR has been reported. In a prospective cohort study we aimed to explore which pathways may contribute to chemotherapy-associated FGR.

Methods: Placental biopsies were collected from 25 cancer patients treated with chemotherapy during pregnancy, and from 66 control patients. Differentially expressed pathways between chemotherapy-exposed patients and controls were examined by whole transcriptome shotgun sequencing (WTSS) and Ingenuity Pathway Analysis (IPA). Immunohistochemical studies for 8-OHdG and eNOS (oxidative DNA damage), proliferation (PCNA) and apoptosis (Cleaved Caspase 3) were performed. The expression level of eNOS, PCNA and IGFBP6 was verified by real-time quantitative Reverse Transcription Polymerase Chain Reaction (RT-qPCR).

Results: Most differential expressed genes between chemotherapy-exposed patients and controls were related to growth, developmental processes, and radical scavenging networks. The duration of chemotherapy exposure had an additional impact on the expression of genes related to the superoxide radicals degeneration network. Immunohistochemical analyses showed a significantly increased expression of 8-OHdG ($P = 0.003$) and a decreased expression of eNOS ($P = 0.015$) in the syncytiotrophoblast of the placenta of cancer patients. A decreased expression of PCNA was detected by immunohistochemistry as RT-qPCR (NS).

Conclusion: Chemotherapy exposure during pregnancy results in an increase of oxidative DNA damage and might impact the placental cellular growth and development, resulting in an increased incidence of FGR in this specific population. Further large prospective cohort studies and longitudinal statistical analyses are needed.

© 2018 Elsevier Ltd. All rights reserved.

1. Introduction

Fetal growth restriction (FGR) can be caused by maternal, placental and fetal factors, or by an imbalance in the complex

* Corresponding author. Center for Gynaecologic Oncology Amsterdam, Antoni van Leeuwenhoek - Netherlands Cancer Institute, Plesmanlaan 121, 1066 CX, Amsterdam, The Netherlands.

E-mail address: f.amant@nki.nl (F. Amant).

interaction between these three compartments [1]. There is evidence to suggest that impaired vasculogenesis is the most striking pathology identified in obstetrical complications and more specifically in FGR [2]. In up to 90% of all growth-restricted infants the underlying cause is placental disturbed angiogenesis and villous formation [3]. Disorders in the very precise elaboration of the uteroplacental compartment may result in an impaired trophoblast invasion and inadequate perfusion, which are known as underlying mechanisms leading to preeclampsia and FGR [4]. Correct diagnosis of FGR is important since FGR carries an increased risk of perinatal morbidity and mortality. Preterm birth, neonatal hypothermia, hypoglycemia, morbidities and even perinatal mortality can occur in the acute setting, while more cardiovascular and metabolic diseases are seen in the long-term follow-up of these children [5–7].

Studies on the outcome of children after prenatal exposure to chemotherapy show an increased risk of FGR [8–12], up to 21%. The high incidence of FGR in pregnant cancer patients may have multiple causes: diminished caloric intake, anemia, increased incidence of thrombosis, toxic (treatment) exposure and negative impact on the uteroplacental blood flow, relative older maternal age, high maternal stress levels, and/or chronic disease/inflammatory response. Animal experiments have shown that tumor growth in pregnant rats has deleterious effects on placenta and fetus [13,14]. Studies reported impaired fetal growth, changes in placental weight and protein content as well as increased hemorrhage and edema with high fetal resorption [13]. It is hypothesized that through competition for nutrients the rapid tumor growth damages the placental development and fetal growth [15]. Substances synthesized by the tumor may cause oxidative stress reactions resulting in an increased ratio of apoptotic trophoblast [14]. In 2009 Abellar R.G. et al. described the pathologic findings in 13 placentas exposed to chemotherapy and observed histologic findings suggestive of placental underdevelopment when chemotherapy was administered during 2nd and 3rd trimesters of pregnancy [16]. However, they also indicated that other detrimental factors (malnutrition, stress, immune suppression) might have had an additional impact.

In this study, we investigated the placental physiology and pathology in a small prospective exploratory cohort study of patients diagnosed and treated for cancer during pregnancy to identify possible mechanisms of chemotherapy-associated FGR. With the use of whole transcriptome shotgun sequencing (WTSS) we explored the presence of important activated or depressed pathways in the placental tissue after chemotherapy-exposure. In addition immunohistochemical and expression analyses by Reverse Transcription Polymerase Chain Reaction (RT-qPCR) were performed to explore some factors related to the differential expressed pathways (oxidative DNA damage, apoptosis, proliferation).

2. Methods

2.1. Patients and data collection

Cancer patients and controls were prospectively recruited during pregnancy. Between January 2014 and September 2016, cancer patients, all treated with chemotherapy during pregnancy, were recruited from Belgium ($n = 19$), the Netherlands ($n = 3$), the Czech Republic ($n = 2$), and Luxembourg ($n = 1$). Controls ($n = 66$) were recruited from the University Hospital Leuven and the University Hospital of Louvain-la-Neuve. All newly registered cancer patients were entered in the study after obtaining a written informed consent; allocation to the FGR or no FGR group took place after delivery. Birth weight percentiles were calculated considering the gestational age at birth, birth weight, sex, ethnicity, parity, and maternal length and weight (www.gestation.net,

v6.7.5.7(NL),2014). A percentile <10 was considered as FGR. FGR controls were recruited based on sonographic Estimated Fetal Weight (EFW) below the 10th percentile, measured after 30 weeks of pregnancy. If after delivery the birth weight percentile turned out to be above 10, the patient was excluded from the FGR control group. Normal weight (NW) controls were recruited at admission to the delivery room. Exclusion criteria for all controls were: maternal medical disorders (Crohn's Disease, colitis, congenital heart disorders, auto-immune disease) and presence of Doppler abnormalities mostly due to early (<30 weeks GA) and severe preeclampsia. The cancer (1) and control (2) patients were subdivided in FGR (A) and NW (B). The study was approved by the Ethical Committee of University Hospital Leuven (Belgian number B322201421061/S56168). Detailed general, obstetric and oncological information was available from the online registry database (www.incipregistration.be) and from patient files. Recorded patient characteristics included maternal age, ethnicity (Caucasian, North-African, African, Asian or Latin-American), maternal body mass index (BMI), cigarette smoking during pregnancy (yes/no), obstetrical complications (including hypertensive disorders, diabetes, preterm labor, maternal infection, or cholestasis (yes/no)), parity (nulli- or multiparous), gender of the neonate, gestational age (GA) at birth (days), birth weight and percentile.

The placentas were weighed immediately after delivery. Placental samples from each patient were taken from 4 different cotyledons (4 quadrants) at the maternal side of the placenta. Each sample was divided in 2 parts and rinsed in phosphate buffered saline (PBS) before storage in RNase buffer (RNA stabilization reagent, Qiagen, Hilden, Germany) and fixation in 4% buffered formaldehyde respectively. Samples in RNase buffer were stored for maximally 4 weeks at 4 °C until analysis. While fixed samples were processed for microscopic examination. All laboratory analyses were performed after validation of the methods and, where possible, samples were tested simultaneously to minimize inter-assay variability.

2.2. RNA extraction from placental tissue, whole transcriptome shotgun sequencing (WTSS) and pathway analysis

Total RNA was isolated using Tripure Isolation Reagent (Sigma-Aldrich, Bornem, Belgium). The quantity of the extracted RNA was photometrically tested (NanoDrop - Isogen Life Science, Temse, Belgium). The quality of the extracted RNA was evaluated by an RNA integrity assay system (Experion RNA StdSens Analyzing kit - Bio-Rad, Nazareth Eke, Belgium: good quality RNA samples included an RNA integrity number > 7 for all samples). One μ g of total RNA was used as input material for sequencing library preparation which was performed with the Illumina TruSeq Stranded mRNA Sample Preparation Kit according to the manufacturers protocol. RNA was denatured at 65 °C in a thermocycler and cooled down to 4 °C. Samples were indexed to allow for multiplexing. Sequencing libraries were quantified using the Qubit fluorometer (Thermo Fisher Scientific, Massachusetts, USA). Library quality and size range was assessed using the Bioanalyser with the DNA 1000 kit (Agilent Technologies, California, USA) according to the manufacturer's recommendations. Each library was diluted to a final concentration of 2 nM and sequenced on Illumina HiSeq2500 according to the manufacturer's recommendations generating 50 bp single-end reads. Adapters from raw reads were filtered with software ea-utils v1.2.2 [17]. Raw reads were aligned to the reference human genome hg19 with Tophat v2.0.13 [18]. Quantification of reads per gene and downstream inference analyses with DeSeq2 [19] were performed using the software Array Studio V10.0 (Qiagen, Hilden, Germany). Fold change of gene expression among different groups, and the corresponding corrected p-value or False

discovery rates, were used to select differentially expressed genes. Cut offs for FDR were set at 0.1. The resulting list of genes were uploaded into Qiagen's Ingenuity Pathway Analysis (IPA) software (Qiagen, Hilden, Germany) to predict possible dysregulated biological pathways.

2.3. Real-time quantitative reverse transcription polymerase chain reaction (RT-qPCR)

cDNA was synthesized (1 µg) using the High-Capacity cDNA Reverse Transcription Kit (Thermo Fisher Scientific, Waltham, Massachusetts, US). The reactions were incubated at 25 °C for 10 min, 37 °C for 120 min, and 85 °C for 5 min and then instantly cooled on ice to 4 °C. 25 ng of input cDNA was used for RT-qPCR analysis. Using TaqMan probes for IGFBP6, eNOS, and PCNA (all from Thermo Fisher Scientific, Waltham, Massachusetts, US), the relative abundance of each target transcript was normalized to the expression level of YWHAZ, UBC, CYC1, and GADPH as endogenous controls and assessed with the Applied Biosystems StepOne Software v2.1. Cycle conditions were: Holding stage of 20 s at 95 °C followed by 40 cycling stages of 1 s at 95 °C and 20 s at 60 °C, for 40 min in total. Critical threshold values of the target genes were normalized to the geometric mean of the 4 endogenous controls and the mean normalized expression of the target genes was calculated using Q-Gene software.

2.4. Immunohistochemistry

Placental tissue samples were fixed for 24 h in 4% buffered formaldehyde, thoroughly rinsed in phosphate-buffered-saline (PBS), brought to ethanol 70% and further processed to paraffin blocks according to standard procedures. Four-µm sections were cut for hematoxylin and eosin (HE) staining and other immunohistochemical studies (8-hydroxy-2'-deoxyguanosine (8-OHdG; marker for oxidative DNA damage), endothelial nitric oxide synthase (eNOS; marker for oxidative stress), proliferating cell nuclear antigen (PCNA; marker for proliferation) and Cleaved Caspase 3 (marker for apoptosis)). For PCNA and eNOS, antigen retrieval was performed by immersion in citrate buffer (pH6) at 90–95 °C for 30 and 60 min respectively. Antigen retrieval for 8-OHdG and Cleaved Caspase 3 was performed in Tris-EDTA buffer (pH9) at 95 °C for 60 and 120 min respectively. Sections were incubated for 2 h (PCNA) or overnight at 4 °C (8-OHdG, eNOS, Cleaved Caspase 3) with the following primary antibodies: 8-OHdG (clone 15A3, 10 µg/ml, Abcam, Cambridge, UK), eNOS (polyclonal ab5589, 10 µg/ml, Abcam, Cambridge, UK), PCNA (clone PC10, 1.635 µg/ml, Agilent Technologies, California, USA) and Cleaved Caspase 3 (polyclonal Asp175, 0.315 µg/ml, Cell Signaling, Massachusetts, US). After incubation with secondary antibodies, binding was visualized with Dako DAB + Chromogen (K3467, Agilent Technologies, California, USA). All sections were counterstained with Harris' hematoxylin. Negative controls were performed by omitting the primary antibody in the first incubation step. To minimize inter-assay variability tissue micro array (TMA) was used. The nuclear staining of 8-OHdG and PCNA was quantified as follows: from each patient, 5 good quality cores were evaluated by counting all positive and negative nuclei in syncytio- and cytotrophoblast respectively and for each core the percentage of positive nuclei was calculated with the following equation [20]:

$$\text{percentage of nuclei}^+ = \frac{\text{no. of nuclei}^+}{\text{no. of nuclei}^+ + \text{no. of nuclei}^-} \times 100$$

then the mean total percentage was calculated per patient.

Similarly the cytoplasmic eNOS and 8-OHdG staining in both trophoblast types were evaluated. Since in the syncytiotrophoblast there are no separate cells, we counted the nuclei which were surrounded by positive staining and calculated their percentage versus the total number of syncytial nuclei for each evaluated field. The endothelial cell layers were scored for circumferential completeness in 5% categories: 0 (absent), 25 (1–25%), 50 (26–50%), 75 (51–75%) and 100 (76–100%). For this, again 5 cores were scored and the total mean percentage was calculated. Throughout the evaluation we used the Zen image analysis system linked to an Axioskop 50 microscope fitted with an Axiocam MRc5 camera (all from Carl Zeiss, Zaventem, Belgium). Photographs were taken at a 25× magnification at the highest resolution possible (2584 × 1936 Pixels).

2.5. Statistical analysis

Median values and range of distribution of continuous variables of the different groups were compared using the Kruskal-Wallis test followed by Dunn's post-test for multiple comparisons and Mann-Whitney *U* test for single comparisons. Non-parametric Mann-Whitney *U* test was used to compare the median of the percentage of positive cells calculated per group between the chemo-exposed placentas and the non-exposed controls. *P*<0.05 was considered statistically significant.

3. Results

A total of 25 cancer patients (10 FGR and 15 NW) and 66 controls (24 FGR and 42 NW) were included. Table 1 shows the recorded patient characteristics of the included patients and controls. There was a statistically significant difference between the distributions of GA at delivery, birth weight, birth percentile, and placental weight between cancer and control groups (Kruskall-Wallis: *P*<0.01). Placental weights were clearly lower in the FGR than in the NW groups, with a median weight of 340 g vs 414 g in cancer patients (Mann-Whitney *U*: *P*=0.015), and 380 g vs 595 g in controls (Mann-Whitney *U*: *P*<0.01).

3.1. Whole transcriptome shotgun sequencing (WTSS)

Different comparisons between the groups were made to explore the differentially expressed genes and their possible relation to FGR after chemotherapy-exposure vs. FGR not related to chemotherapy (Supplementary appendix, Tables 1a–1c, Fig. 1a). Comparing the chemotherapy-exposed groups (1A-B) with the control groups (2A-B), 69 out of 20314 genes were significantly up- or downregulated ($\text{FC} \geq 1.5$ or ≤ -1.5 ; $\text{FDR} \leq 0.1$). Out of these 69 genes, only one was downregulated, C-type lectin domain family 4, member M (CLEC4M). In Table 2 we show the 10 most dysregulated genes. Most genes were associated to the following 5 network functions: cellular development, cellular growth and proliferation, organ development, cell-to-cell signaling and interaction, and inflammatory response. Comparing the FGR groups and NW groups exposed or not exposed to chemotherapy, 161 genes were significantly up- or downregulated between 1A and 2A but only 7 genes between 1B and 2B. Associated network functions were: cellular movement, tissue development, cardiovascular system development and function, free radical scavenging, and small molecule biochemistry. We compared the highest dysregulated genes ($\text{FC} \geq 1.5$ or ≤ -1.5) from the comparisons of chemotherapy-exposed patients vs the NW controls (1A vs 2B and 1B vs 2B) and observed that only 2 genes were concordant: poly(A) binding protein, cytoplasmic 3 (PABPC3) and delta-aminolevulinate synthase 2 (ALAS2) (Supplementary appendix, Fig. 1c). Two genes

Table 1
Recorded patient characteristics.

	Chemotherapy; FGR (n = 10) (Group 1A)	Chemotherapy; no FGR (n = 15) (Group 1B)	No cancer; FGR (n = 24) (Group 2A)	No cancer; no FGR (n = 42) (Group 2B)	P Value (between all groups)
Age (Yr): median [range]	33 (25–39)	31 (22–36)	30 (22–42)	31 (18–41)	0.465
BMI: median [range]	25.6 (18.7–29.4)	24.1 (16.4–35.9)	22.0 (18.6–28.7)	21.6 (16.9–38.3)	0.101
Parity: nulli-multi	3–7	8–7	13–11	17–25	
Ethnicity					
Caucasian	9	14	20	34	
North-African	1	1	2	2	
African			1	2	
Latin-American				1	
Asian			1	3	
Smoking: y-n	1–9	1–14	5–19	3–39	
GA (days) at delivery: median [range]	261 (240; 270)	261 (215; 272)	262 (217; 277)	274 (243; 288)	<0.01
Type of delivery: vaginal Cesarean section	5–5	10–5	12–12	27–15	
Gender child: male-female	7–3	8–7	8–16	20–22	
Birth Weight (g): median [range]	2395 (1880; 2820)	2735 (1600; 3360)	2275 (1370; 2750)	3285 (2380; 4110)	<0.01
Birth Percentile: median [range]	2.9 (0.1; 8.6)	29.2 (11.8; 74.6)	2.6 (0.01; 9.3)	42.9 (10.1; 95.8)	<0.01
Placental Weight (g) (median; range) ^a	340 (211–440)	414 (252–640)	380 (161–580)	595 (390–800)	<0.01
Obstetrical complications					
Hypertensive disorders ^b : y-n	1–9		4–20	3–39 ^c	
Gestational diabetes ^b : y-n	2–8	1–14 ^c		3–39 ^c	
Cholestasis: y-n		1–14 ^c			
GA (days) at diagnosis: median [range]	126 (20; 185)	140 (19; 217)			
Tumor type					
Breast	6	10			
Lymphoma: HL-NHL	4; 0–4	1: 1–0			
Leukemia		1			
Brain		1			
Gastro-intestinal		2			
Cancer Treatment					
Surgery + CT	4	5			
CT	2	8			
CT + RT	0	1			
CT + targeted therapy (Rituximab)	4	1			
GA (days) at start chemotherapy: median [range]	131 (91; 198)	163 (92; 222)			
GA (days) at end chemotherapy: median [range]	235 (220; 260)	242 (190; 259)			
Type of chemotherapy: n; median number of cycles [range]					
Alkylating agents	10; 4 (1; 6)	12; 3 (2; 7)			
Anthracyclines	10; 4 (1; 6)	12; 3 (1; 7)			
Taxanes	4; 3 (3; 12)	5; 8 (3; 11)			
Platinum-based	/	2 (3; 5)			
Vinca Alkaloids	4; 4 (4; 6)	1 (7)			
Antimetabolites	4; 3 (3; 4)	6; 3 (1; 6)			
Targeted Therapy	4; 5 (4; 6)	/			

Abbreviations: FGR = Fetal Growth Restriction; GA = Gestational Age; BMI = Body Mass Index; HL = Hodgkin lymphoma; NHL = non-Hodgkin Lymphoma; CT = Chemotherapy; RT = Radiotherapy; y = yes; n = no; NS = not significant.

^a Data available of respectively 9, 9, 20 and 34 placentas of the different groups.

^b In any of the included patients, medication was required. No patient was diagnosed with preeclampsia.

^c In one patient 2 complications were registered.

involved in (mRNA) metabolism. Exploring more specifically the differences between FGR related to chemotherapy exposure and FGR without exposure, we compared group 1A and 1B, and 2A and 2B, but no significantly up- or downregulated genes ($FC \geq 1.5$ or ≤ -1.5 ; $FDR \leq 0.1$) were observed. To assess if other factors besides chemotherapy could be related to the increased incidence of FGR after chemotherapy-exposure, we explored the differences in cancer types (breast cancer vs hematological malignancies), trimester at diagnosis, maternal age and delivery mode (vaginal birth vs cesarean section). The start of chemotherapy had an additional impact on the gene expression, with 86 genes significantly differential expressed between early start of exposure (<196 days GA) and late start of exposure (>196 days GA) (Supplementary appendix, Table 1d). One of the network functions in which these

genes were involved is the superoxide radicals degeneration network. For all other comparisons no significantly differential expressed genes were observed.

3.2. Immunohistochemistry

We were specifically interested in exploring the effect of chemotherapy on the oxidative DNA damage, proliferation and apoptosis. By immunohistochemical analyses we explored the expression of 8-OHdG, eNOS, PCNA and Cleaved Caspase 3. The quantitative data are shown in Table 3.

There was significantly more nuclear expression of 8-OHdG in the trophoblast of the placentas in groups 1A and B vs groups 2A and B ($P=0.003$) (Fig. 1). In the FGR control placentas (group 2A) the

Table 2

Highest statistically significant down- and upregulated genes between patients (1A-B) and controls (2A-B). The 5 most network functions associated to the dysregulated genes between all chemotherapy exposed and control cases were: cellular development, cellular growth and proliferation, organ development, cell-to-cell signaling and interaction, and inflammatory response. The networks for the subanalysis of FGR cases were: cellular movement, tissue development, cardiovascular system development and function, free radical scavenging, and small molecule biochemistry. A positive respectively negative FC means up- and downregulated in the chemotherapy-exposed placentas. IPA: Ingenuity Pathway Analysis, FC: fold change, FDR: false discovery rate, FGR: fetal growth restriction.

IPA name	Full name	Main function	1A-B vs 2A-B		1A vs 2A	
			FC	FDR	FC	FDR
CLEC4M	C-type lectin domain family 4, member M	transmembrane receptor, involved in the immune system, probable pathogen-recognition receptor	-1.53	<0.01		
HBB	hemoglobin, beta	the hemoglobin chains, each with its own heme moiety, cooperate in binding and release of oxygen	1.81	<0.01		
HBQ1	hemoglobin, theta 1	found in human foetal erythroid tissue, research supports a transcriptionally active role possibly in early erythroid tissue	1.73	<0.01		
IGFBP6	insulin-like growth factor binding protein 6	modulates IGF-mediated growth and developmental rates	1.69	<0.01		
ALAS2	aminolevulinate, delta-, synthase 2	erythroid-specific mitochondrially located enzyme, catalyzes the first step in the heme biosynthetic pathway	1.67	<0.01		
HBG2	hemoglobin, gamma G	gamma globin genes are normally expressed in the foetal liver, spleen and bone marrow, together with two alpha chains constitute foetal hemoglobin (HbF)	1.66	<0.01		
S100A4	S100 calcium binding protein A4	localized in the cytoplasm and/or nucleus of a wide range of cells, involved in the regulation of cell cycle progression and differentiation	1.66	<0.01		
ANKRD1	ankyrin repeat domain 1 (cardiac muscle)	localized to the nucleus of endothelial cells, induced by IL-1 and TNF- α stimulation, functions as a transcription factor in endothelial cell activation	1.66	<0.01		
HBA1	hemoglobin, alpha 1	the hemoglobin chains, each with its own heme moiety, cooperate in binding and release of oxygen	1.65	<0.01		
MMP7	matrix metallopeptidase 7 (matrilysin, uterine)	proteins in this family are involved in the breakdown of extracellular matrix in normal physiological processes (embryonic development, reproduction, tissue remodeling), as well as in disease processes (arthritis, metastasis)	1.65	<0.01		
ADORA3	adenosine A3 receptor	belongs to the family of G-protein-coupled receptors involved in a variety of intracellular signaling pathways and physiological functions, mediates both cell proliferation and cell death	1.64	<0.01		
KLHL14	kelch-like family member 14	member of the Kelch-like gene family, cell cycle regulators, play a role in mitosis	-1.69	0.08		
LRP2	low density lipoprotein receptor-related protein 2	critical for the reuptake of lipoproteins, sterols, vitamin-binding proteins, and hormones, but also has a role in cell-signaling processes	-1.68	0.03		
SLC4A4	solute carrier family 4 (sodium bicarbonate cotransporter), member 4	encodes a sodium bicarbonat cotransporter, also related to other transport pathways (glucose, bile salts and organic acids, metal ions and amine compounds)	-1.63	0.10		
NRXN3	neurexin 3	neuronal cell surface protein that may be involved in cell recognition and cell adhesion, may mediate intracellular signaling and may play a role in angiogenesis	-1.62	0.09		
F5	coagulation factor V (proaccelerin, labile factor)	central regulator of hemostasis, critical cofactor for activated factor Xa resulting in the activation of prothrombin to thrombin	-1.61	0.06		
FBXO27	F-box protein 27	member of the F-box protein family, interact with ubiquitination targets through other protein interaction domains, related to the immune system pathway	-1.58	0.09		
GLUD2	glutamate dehydrogenase 2	acts as a homohexamer to recycle glutamate during neurotransmission	-1.57	0.10		
KDR (VEGFR2)	kinase insert domain receptor (vascular endothelial growth factor receptor 2)	promotes proliferation, survival, migration and differentiation of endothelial cells, required for VEGFA-mediated induction of NOS2 and NOS3, leading to the production of the signaling molecule nitric oxide (NO) by endothelial cells	-1.55	0.10		
PMAIP1	phorbol-12-myristate-13-acetate-induced protein 1	promotes activation of caspases and apoptosis, contributes to p53/TP53-dependent apoptosis after radiation exposure	-1.52	0.10		
LAMA2	laminin, alpha 2	thought to mediate the attachment, migration, and organization of cells into tissues during embryonic development by interacting with other extracellular matrix components	-1.51	0.09		
CRIP1	cysteine-rich protein 1 (intestinal)	role in zinc absorption, may function as an intracellular zinc transport protein	1.94	0.03		
C19orf33	chromosome 19 open reading frame 33	found primarily in the nucleus, may play a role in placental development and diseases such as pre-eclampsia	1.93	0.03		
ATOH8	ataonal homolog 8 (Drosophila)	regulates endothelial cell proliferation, migration and tube-like structures formation, modulates endothelial cell differentiation through NOS3 (eNOS)	1.93	0.03		
ST6GAL2	ST6 beta-galactosamidase alpha-2,6-sialyltransferase 2	involved in the generation of the cell-surface carbohydrate determinants	1.90	0.04		
HES4	hes family bHLH transcription factor 4	transcriptional repressor, negative regulator of myogenesis, may play a role in response pathways to DNA cross-link damage	1.87	0.05		
SPON2	spondin 2, extracellular matrix protein	cell adhesion protein, promotes adhesion and outgrowth of hippocampal embryonic neurons	1.86	0.05		
B3GNT8	UDP-GlcNAc:betaGal beta-1,3-N-acetylglucosaminyltransferase 8	plays a role in the elongation of specific branch structures of multiantennary N-glycans	1.82	0.03		
FXYD1			1.82	0.06		

(continued on next page)

Table 2 (continued)

IPA name	Full name	Main function	1A-B vs 2A-B		1A vs 2A	
			FC	FDR	FC	FDR
IFITM10	FXYD domain containing ion transport regulator 1 interferon induced transmembrane protein 10	regulated ion channel activity, may have a functional role in muscle contraction IFN-induced antiviral protein which disrupts intracellular cholesterol homeostasis, inhibits the entry of viruses to the host cell cytoplasm by preventing viral fusion with cholesterol depleted endosomes			1.82	0.06
ADRA2C	adrenoceptor alpha 2C	member of the G protein-coupled receptor superfamily, have a critical role in regulating neurotransmitter release			1.81	0.06

Table 3

Quantitative evaluation of 8-OHdG, eNOS and PCNA: minimum (min), maximum (max), median and interquartile range (IQR) of the percentages of positive trophoblasts or endothelial cells were shown (Mann-Whitney *U* test). For Cleaved Caspase 3 the total number of positive cytrophoblast was low in all groups. Of all evaluated cores per placenta we calculated in total respectively 1 to 6 positive cytrophoblasts (group 1A); 0 to 14 (group 1B); 0 to 8 (group 2A); and 0 to 9 (group 2B). 1A = chemotherapy-exposed with FGR; 1B = chemotherapy-exposed with NW; 2A = FGR control; 2B = NW control. *P < 0.05 is considered significant. Abbreviations: FGR= Fetal Growth Restriction, NW= Normal Weight.

Staining	Parameters	Group 1A (n = 10)	Group 1B (n = 15)	Group 2A (n = 24)	Group 2B (n = 42)	P-value (group 1A vs 2A)	P-value (group 1B vs 2B)	P-value (group 1A-B vs 2A-B)
8-OHdG (nuclear/cytoplasmic, trophoblast)	Min	48.0	24.0	5.2	10.0	0.061	0.044*	0.003*
	Median	86.8	90.6	62.5	58.0			
	Max	100.0	100.0	100.0	100.0			
	IQR	40.0	61.0	63.5	33.6			
eNOS (cytoplasmic, endothelial cells)	Min	0.0	15.0	0.0	0.0	0.940	0.358	0.702
	Median	72.5	30.0	57.5	45.0			
	Max	95.5	100.0	100.0	100.0			
	IQR	56.0	35.0	50.0	40.0			
eNOS (cytoplasmic, syncytiotrophoblast)	Min	0.0	0.0	4.0	0.0	0.066	0.102	0.015*
	Median	45.0	34.0	64.5	64.0			
	Max	96.0	86.0	100.0	99.0			
	IQR	66.0	78.0	42.0	54.0			
PCNA (nuclear, cytrophoblast)	Min	0.2	0.4	2.2	0.6	0.076	0.710	0.135
	Median	11.0	12.6	15.7	20.1			
	Max	21.2	72.0	58.0	81.0			
	IQR	18.4	38.4	19.2	37.0			

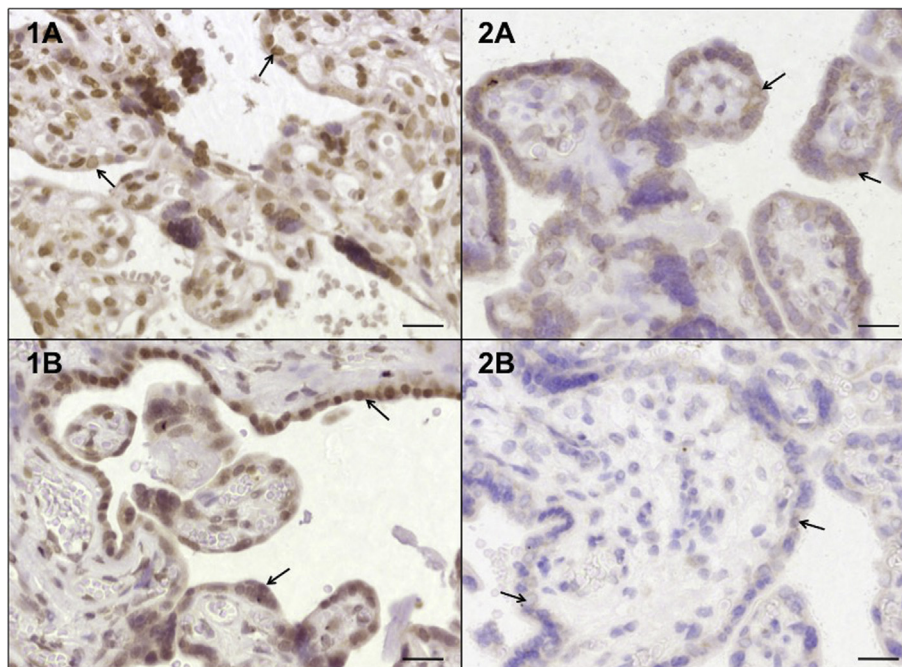


Fig. 1. Expression of 8-OHdG indicating DNA damage in chemotherapy-exposed placental tissue with FGR (1A), chemotherapy-exposed with NW (1B), control FGR (2A), and control NW (2B). Arrows point at the trophoblastic layers. Images were taken at 25× magnification. Scalebar = 20 μm.

nuclear expression of 8-OHdG was clearly lower, but there was marked cytoplasmic staining which was probably due to the presence of mitochondrial DNA damage [21]. Most of the normal weight controls (group 2B) had very limited expression of 8-OHdG.

While the expression of eNOS in the endothelial cells of the groups 1A and B was high and comparable to the expression in groups 2A and B ($P=0.702$) (Fig. 2), the expression of eNOS in the syncytiotrophoblast of groups 1A and B was significantly lower when compared to groups 2A and B ($P=0.015$).

PCNA immunoreactivity was present in villous cytotrophoblast of all groups (Fig. 3). We observed a decreased percentage of positive cells in groups 1A and B vs groups 2A and B ($P=0.135$). In our observation FGR placentas showed lower expression compared to the controls without FGR, but this was not statistically significant (data not shown).

The rate of apoptosis as detected by the expression of Cleaved Caspase 3 showed a very limited expression in all groups.

3.3. Real-time quantitative reverse transcription polymerase chain reaction (RT-qPCR)

We verified the immunohistochemical expression of eNOS and PCNA by RT-qPCR. The expression of eNOS by RT-qPCR showed comparable results between both groups ($P=0.804$) (Fig. 4). The decreased percentage of proliferation (PCNA) was confirmed by RT-qPCR ($P=0.175$) (Fig. 4).

To verify the expression levels observed by WTSS, we verified by RT-qPCR the significant upregulation of IGFBP6, being an important factor in growth processes. A comparable significant upregulation ($P=0.001$) was observed (Fig. 4).

4. Discussion

Whole transcriptome sequencing and immunohistochemical analysis revealed an increase in oxidative DNA damage, which might impact the growth and developmental processes in chemotherapy-exposed placentas compared to placentas of healthy pregnancies. Genes connected to the oxidative damage pathway were more expressed in chemotherapy-exposed as well as in the

control FGR placentas with an increased expression of the oxidative DNA damage marker 8-OHdG in the trophoblast. No increased rate of apoptosis could be detected.

The etiology underlying FGR is divided in three groups with maternal, fetal or placental factors involved. Up to 90% of events is caused by placental dysfunction, which may result from abnormal placental bed development with poor spiral artery remodeling, physical separation at the maternal interface, or from dysregulated metabolic adaptations [22–24]. The placental weight was shown to be lower in growth restricted fetuses [25] and also in our study lower placental weights were recorded in the FGR groups. This lower placental weight in the cancer patients might indicate a potential negative impact caused by the tumor growth, chemotherapeutic agents or other detrimental factors (malnutrition, stress, immune suppression) on the placental development.

WTSS and IPA analysis revealed different processes that might be involved to the increased incidence of FGR in chemotherapy-exposed pregnancies. Most differentially expressed genes between chemotherapy-exposed and controls were related to growth and developmental processes, and radical scavenging networks. Comparative analyses between the FGR and no FGR cases in both the chemotherapy-exposed and control groups, did not reveal statistically significant differentially expressed genes. Therefore we cannot describe a causal link between the differential gene expression and FGR. We compared some other variables to investigate if these factors might be contributive to the increased incidence of FGR. We observed that the duration of chemotherapy exposure had an additional impact on the expression of genes related to superoxide radicals degeneration. Because in the FGR cases the median start of treatment was earlier than in the NW cases (131 days vs 163 days) and also the duration of chemotherapy was longer (104 days vs 76 days). This adds to our hypothesis that chemotherapy exposure might be the dominant factor towards the increased incidence of FGR in pregnant cancer patients. Large-scale longitudinal comparative analyses on the expression levels of genes would however be more informative. No significantly dysregulated genes were found when we compared different cancer types (breast cancer vs hematological malignancies), maternal age, maternal BMI, and delivery mode (vaginal birth vs cesarean section).

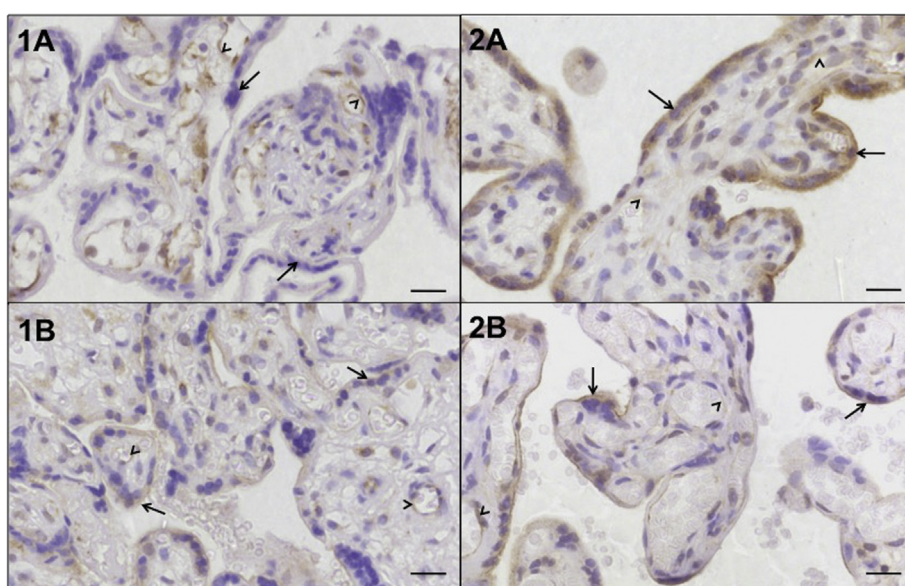


Fig. 2. Expression of eNOS in chemotherapy-exposed placental tissue with FGR (1A), chemotherapy-exposed with NW (1B), control FGR (2A), and control NW (2B). Arrowheads indicate the fetal endothelial cells; arrows point at the trophoblastic layers. Images were taken at 25 \times magnification. Scalebar = 20 μ m.

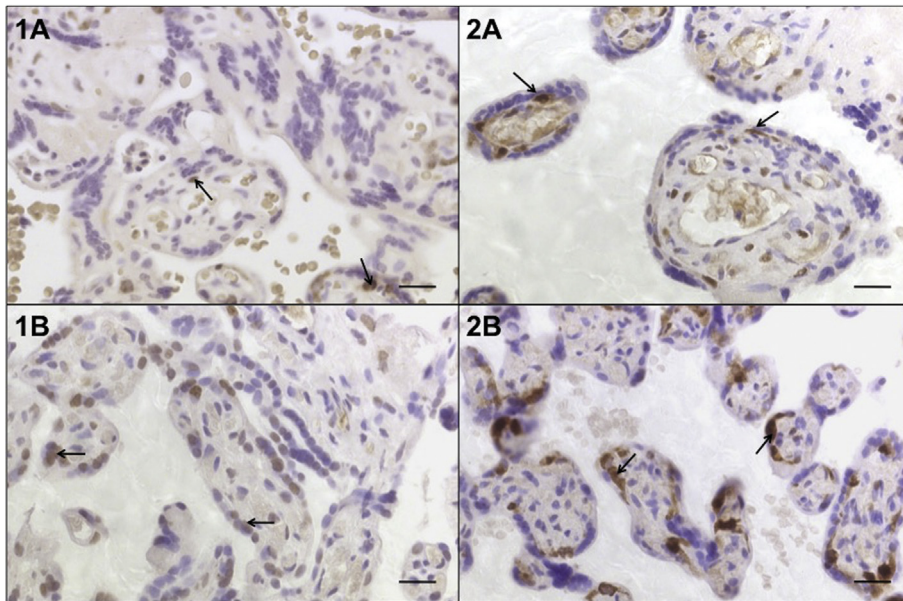


Fig. 3. Expression of PCNA in chemotherapy-exposed placental tissue with FGR (1A), chemotherapy-exposed with NW (1B), control FGR (2A), and control NW (2B). Arrows point at the cytotrophoblast. Images were taken at 25 \times magnification. Scalebar = 20 μ m.

Normal physiological conditions in aerobic organisms provide a balance between endogenous oxidants, which lead to tissue damage, and several enzymatic and non-enzymatic mechanisms of tissue defense. Imbalances between these processes will lead to extensive oxidative damage. DNA damage leads to the formation of several DNA products. Among them is a hydroxyl product of deoxyguanosine generated in vivo by oxidative damage, which can be measured quantitatively as 8-OHdG lesions, both nuclear and cytoplasmic (mitochondrial DNA damage) [21,26]. Previous studies already mentioned the presence of this marker in pregnancies complicated by preeclampsia and FGR [27,28]. In the present study

an increase of 8-OHdG expression in the cyto- and syncytiotrophoblast was present in the chemotherapy-exposed groups ($P=0.003$). This might be indicative for direct toxicity of the chemotherapeutic agents to the trophoblast layers.

WTSS revealed an increased association to the radical scavenging function in FGR after chemotherapy-exposure. The nitric oxide radical is generated from the metabolism of L-arginine by the enzyme nitric oxide synthase (NOS) in the endothelium, which diffuses into the underlying vascular smooth muscle and by its activation of guanylate cyclase, leads to vascular relaxation [29]. There are three isoforms of NOS: neuronal (nNOS), endothelial

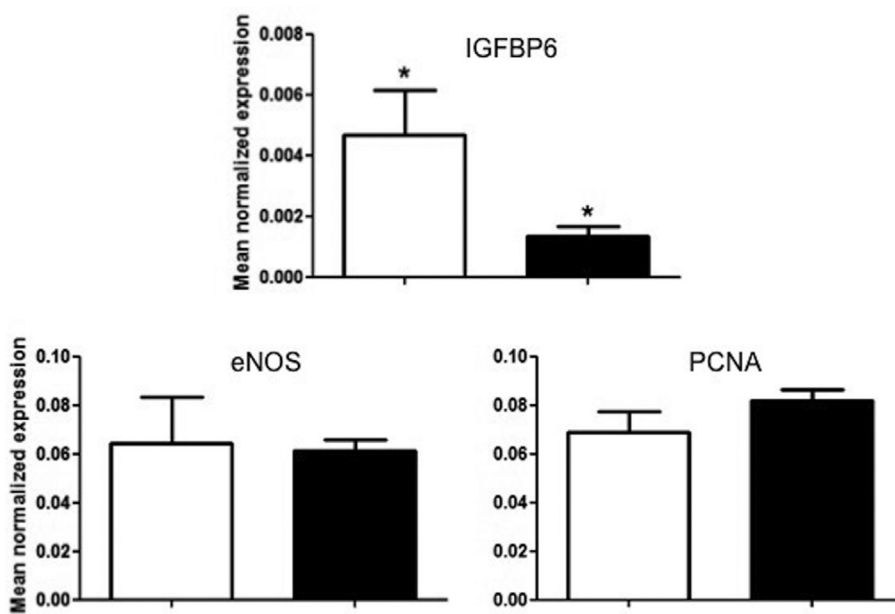


Fig. 4. Mean normalized expression of CT values of IGFBP6, eNOS and PCNA in the placental tissue of chemotherapy-exposed patients (white bar) and non-exposed control patients (black bar). Data are expressed as mean + standard error of the mean (SEM). There was a statistically significant difference between both groups for the expression of IGFBP6 (*).

(eNOS) and inducible (iNOS), of which the latter two are expressed in the placenta, mainly in syncytiotrophoblast and endothelial cells. iNOS peaks at mid gestation whereas eNOS expression increases towards the end of the third trimester [30,31]. The main stimulus for NO release in placental vessels and for angiogenesis via eNOS activation is shear stress (frictional force between blood flow and endothelium) [30]. Although not statistically significant, we observed an increased expression of eNOS in the endothelial cells between chemotherapy-exposed placentas and controls, but significantly lower expression of eNOS in the syncytiotrophoblast ($P=0.015$) and comparable levels assessed by RT-qPCR (NS). Oxidative stress has been related to a decreased activity and expression of eNOS in the fetal endothelial cells, impairing the NOS-dependent relaxation [32], compared to an increased expression at the trophoblast activating the pathologic angiogenesis [3]. Our results indicate that no increased oxidative stress (as evaluated by the expression of eNOS at the DNA and protein level) is present in the fetal endothelial cells and syncytiotrophoblast after chemotherapy exposure. However, earlier Toledo et al. described the increase of the malondialdehyde content as an oxidative stress biomarker in the placentas of tumor-bearing rats [14].

IGFBP1 has been described as negatively correlated with birth and placental weight [33]. By WTSS and verified by RT-qPCR, we revealed a significant upregulation of IGFBP6 in the chemotherapy-exposed placentas ($P=0.001$). Up till now, no data are published on the expression levels of IGFBP6 in the placenta and its possible correlation with birth weight. Investigating the expression of IGF's and IGFBP's in our specific patient population would therefore be very interesting.

We used PCNA as a commonly used proliferation marker to examine the effect of chemotherapy on the cellular proliferation processes. In the human placenta, the most intense expression of PCNA has been identified in villous and invasive cytotrophoblasts [34] with lower expression seen in FGR placentas [35]. We noticed a decreased expression of PCNA (IHC and RT-qPCR) in the chemotherapy-exposed placentas vs the controls (NS). Apoptosis was not increased in the chemotherapy-exposed placentas as observed by the limited expression of Cleaved Caspase 3. Elmore described the complexity of apoptosis and its different interacting pathways [36]. The intrinsic, extrinsic and perforin/granzyme pathways all contribute to DNA degradation and cleavage, but not all of them activate caspases. Therefore we speculate that in the placental tissues studied, the caspase-pathway may not have been involved in apoptosis.

There are some limitations in this study. Most importantly, the groups are small with only 10 cases of FGR in the patients exposed to chemotherapy. Additional comparative analyses between potential confounding variables (cancer types, start of treatment, maternal age and BMI, delivery mode) showed that a longer treatment exposure has an additional impact on the differential expression of 86 genes of which a number was related to the network of superoxide radicals degeneration. Despite these extended comparative analyses, there is still a large heterogeneity in the therapeutic agents, and number of cycles administered within the study groups. Although we could not detect significant differentially expressed genes between the breast cancer patients compared to the hematologic malignancies, 4 patients of the FGR group had a hematologic malignancy whereas only 1 patient in the NW group. This might still suggest that the kind of malignancy (local vs systemic) influences fetal growth. Additionally, we cannot exclude the effect of maternal habits during the course of pregnancy (smoking [37], alcohol intake, stress [38] or other toxic exposures) affecting the placenta and its expression of different markers/genes.

5. Conclusion

This is the first case cohort study exploring the effects of cancer and chemotherapy on the placental tissue, investigating placental changes and underlying mechanisms for FGR. Here we observed that the placental tissue of cancer patients treated with chemotherapy shows an increase in oxidative DNA damage. This might have an impact on the placental cellular growth and development. Early start of chemotherapy treatment and a longer exposure resulted in increased incidence of FGR. To examine whether this increased oxidative DNA damage explains the increased incidence of FGR, larger prospective cohort studies are required.

Conflicts of interest

All authors declare that they participated in the study (inclusion of patients (IB, MMG, MH, LL); RNA-extraction, WTSS and IPA analyses (RVB, VB, ACC, JFF, JV); immunohistochemistry (GV, TE)). All final analyses and first draft of the manuscript were made by MV, and corrected by FA and KVC. All authors have seen and approved the final version. None declared any conflicts of interest. (COI forms of all authors provided)

Funding

This study was supported by the gs1:Research Foundation Flanders (senior clinical investigator grant to Prof. Dr. Amant and fellowships to Dr. Verheecke), the European Research Council (CRADLE consolidator grant, grant no. ZKD0230, to Prof. Dr. Amant), and the Charles University research Progress Q28-Oncology (grant to Prof. Dr. Halaska).

Acknowledgements

We thank Marloes Rood for her help with the immunohistochemical studies and Lisbeth Vercruyse for the evaluation of the microscopic imaging.

Appendix A. Supplementary data

Supplementary data related to this article can be found at <https://doi.org/10.1016/j.placenta.2018.03.002>.

References

- [1] F.G. Cunningham, Fetal growth disorders, in: F.G. Cunningham, K.J. Leveno, S.L. Bloom, J.C. Hauth, D.J. Rouse, C.Y. Spong (Eds.), *Williams Obstetrics*, 23rd ed., US: McGraw-Hill, New York, 2010, pp. 842–858.
- [2] D.B. Chen, J. Zheng, Regulation of placental angiogenesis, *Microcirculation* 21 (2014) 15–25.
- [3] F. Barut, A. Barut, B.D. Gun, N.O. Kandemir, M.I. Harma, M. Harma, E. Aktunc, S.O. Ozdamar, Intrauterine growth restriction and placental angiogenesis, *Diagn. Pathol.* 5 (2010) 24.
- [4] S. Kwiatkowski, B. Dolęgowska, E. Kwiatkowska, R. Rzepka, A. Torbè, M. Bednarek-Jędrzejek, A common profile of disordered angiogenic factor production and the exacerbation of inflammation in early preeclampsia, late preeclampsia, and intrauterine growth restriction, *PLoS One* 11 (2016) e0165060.
- [5] D. Maulik, Fetal growth compromise: definitions, standards, and classification, *Clin. Obstet. Gynecol.* 49 (2006) 214–218.
- [6] F. Figueras, E. Gratacos, An integrated approach to fetal growth restriction, *Best Pract. Res. Clin. Obstet. Gynaecol.* 38 (2017) 48–58.
- [7] E.K. Pallotto, H.W. Kilbride, Perinatal outcome and later implications of intrauterine growth restriction, *Clin. Obstet. Gynecol.* 49 (2006) 257–269.
- [8] K. Van Calsteren, L. Heyns, F. De Smet, L. Van Eycken, M.M. Gziri, W. Van Gemert, M. Halaska, I. Vergote, N. Ottevanger, F. Amant, Cancer during pregnancy: an analysis of 215 patients emphasizing the obstetrical and the neonatal outcomes, *J. Clin. Oncol.* 28 (2010) 683–689.
- [9] F. Amant, K. Van Calsteren, M.J. Halaska, M.M. Gziri, W. Hui, L. Lagae, M.A. Willemse, L. Kapusta, B. Van Calsteren, H. Wouters, L. Heyns, S.N. Han, V. Tomek, L. Mertens, P.B. Ottevanger, Long-term cognitive and cardiac

- outcomes after prenatal exposure to chemotherapy in children aged 18 months or older: an observational study, *Lancet Oncol.* 13 (2012) 256–264.
- [10] B. Weisz, E. Schiff, M. Lishner, Cancer in pregnancy: maternal and fetal implications, *Hum. Reprod. Update* 7 (2001) 384–393.
- [11] D. Fischer, A. Ahr, B. Schaefer, A. Veldman, R. Schloesser, Outcome of preterm and term neonates of mothers with malignant diseases diagnosed during pregnancy, *J. Matern. Fetal Neonatal Med.* 19 (2006) 101–103.
- [12] E. Cardonick, A. Iacobucci, Use of chemotherapy during human pregnancy, *Lancet Oncol.* 5 (2004) 283–291.
- [13] M.T. Toledo, G. Ventrucci, M.C. Marcondes, Cancer during pregnancy alters the activity of rat placenta and enhances the expression of cleaved PARP, cytochrome-c and caspase 3, *BMC Canc.* 6 (2006) 168.
- [14] M.T. Toledo, G. Ventrucci, M.C. Gomes-Marcondes, Increased oxidative stress in the placenta tissue and cell culture of tumour-bearing pregnant rats, *Placenta* 32 (2011) 859–864.
- [15] M. Gomes-Marcondes, L C, R C, Consequences of Walker tumour growth for the placental/foetal development in rats, *Cancer Res Ther Con* 5 (1998) 277–283.
- [16] R.G. Abellar, J.R. Pepperell, D. Greco, F. Gundogan, S. Kostadinov, J. Schwartz, U. Tantravahi, M.E. De Paep, Effects of chemotherapy during pregnancy on the placenta, *Pediatr. Dev. Pathol.* 12 (2009) 35–41.
- [17] E. Aronesty, EA-utils: command-line tools for processing biological sequencing data. <https://github.com/ExpressionAnalysis/ea-utils>, 2011.
- [18] D. Kim, G. Pertea, C. Trapnell, H. Pimentel, R. Kelley, S.L. Salzberg, TopHat2: accurate alignment of transcriptomes in the presence of insertions, deletions and gene fusions, *Genome Biol.* 14 (2013). R36.
- [19] S. Anders, W. Huber, Differential expression analysis for sequence count data, *Genome Biol.* 11 (2010). R106.
- [20] M. Galton, DNA content of placental nuclei, *J. Cell Biol.* 13 (1962) 183–191.
- [21] K. Nomoto, K. Tsuneyama, H. Takahashi, Y. Murai, Y. Takano, Cytoplasmic fine granular expression of 8-hydroxydeoxyguanosine reflects early mitochondrial oxidative DNA damage in nonalcoholic fatty liver disease, *Appl. Immunohistochem. Mol. Morphol.* 16 (2008) 71–75.
- [22] S. Sankaran, P.M. Kyle, Aetiology and pathogenesis of IUGR, *Best Pract. Res. Clin. Obstet. Gynaecol.* 23 (2009) 765–777.
- [23] D. Maulik, J. Frances Evans, L. Ragolia, Fetal growth restriction: pathogenic mechanisms, *Clin. Obstet. Gynecol.* 49 (2006) 219–227.
- [24] D. Newbern, M. Freemark, Placental hormones and the control of maternal metabolism and fetal growth, *Curr. Opin. Endocrinol. Diabetes Obes.* 18 (2011) 409–416.
- [25] S. Heinonen, P. Taipale, S. Saarikoski, Weights of placentae from small-for-gestational age infants revisited, *Placenta* 22 (2001) 399–404.
- [26] A. Valavanidis, T. Vlachogianni, C. Fiotakis, 8-hydroxy-2'-deoxyguanosine (8-OHdG): a critical biomarker of oxidative stress and carcinogenesis, *J. Environ. Sci. Health C Environ. Carcinog. Ecotoxicol. Rev.* 27 (2009) 120–139.
- [27] A. Fujimaki, K. Watanabe, T. Mori, C. Kimura, K. Shinohara, A. Wakatsuki, Placental oxidative DNA damage and its repair in preeclamptic women with fetal growth restriction, *Placenta* 32 (2011) 367–372.
- [28] Y. Takagi, T. Nikaido, T. Toki, N. Kita, M. Kanai, T. Ashida, S. Ohira, I. Konishi, Levels of oxidative stress and redox-related molecules in the placenta in preeclampsia and fetal growth restriction, *Virchows Arch.* 444 (2004) 49–55.
- [29] B.J. Krause, M.A. Hanson, P. Casanello, Role of nitric oxide in placental vascular development and function, *Placenta* 32 (2011) 797–805.
- [30] S.A. Baylis, P.J. Strijbos, A. Sandra, R.J. Russell, A. Rijhsinghani, J.G. Charles, C.P. Weiner, Temporal expression of inducible nitric oxide synthase in mouse and human placenta, *Mol. Hum. Reprod.* 5 (1999) 277–286.
- [31] J. Dötsch, N. Hogen, Z. Nyúl, J. Hänze, I. Knerr, M. Kirschbaum, W. Rascher, Increase of endothelial nitric oxide synthase and endothelin-1 mRNA expression in human placenta during gestation, *Eur. J. Obstet. Gynecol. Reprod. Biol.* 97 (2001) 163–167.
- [32] U. Förstermann, Nitric oxide and oxidative stress in vascular disease, *Pflügers Archiv* 459 (2010) 923–939.
- [33] J. Verhaeghe, W. Coopmans, E. Van Herck, D. Van Schoubroeck, J.A. Deprest, I. Witters, IGF-I, IGF-II, IGF binding protein 1, and C-peptide in second trimester amniotic fluid are dependent on gestational age but do not predict weight at birth, *Pediatr. Res.* 46 (1) (1999) 101–108.
- [34] L. Danihel, P. Gomolcák, M. Korbel, J. Pruzinec, J. Vojtassák, P. Janík, P. Babál, Expression of proliferation and apoptotic markers in human placenta during pregnancy, *Acta Histochem.* 104 (2002) 335–338.
- [35] G. Unek, A. Ozmen, M. Ozekinci, M. Sakinci, E.T. Korgun, Immunolocalization of cell cycle proteins (p57, p27, cyclin D3, PCNA and Ki67) in intrauterine growth retardation (IUGR) and normal human term placentas, *Acta Histochem.* 116 (2014) 493–502.
- [36] S. Elmore, Apoptosis: a review of programmed cell death, *Toxicol. Pathol.* 35 (2007) 495–516.
- [37] S. Sabra, E. Gratacós, M.D. Gómez Roig, Smoking-induced changes in the maternal immune, endocrine, and metabolic pathways and their impact on fetal growth: a topical review, *Fetal Diagn. Ther.* 41 (2017) 241–250.
- [38] T.H. Hung, S.F. Chen, T.T. Hsieh, L.M. Lo, M.J. Li, Y.L. Yeh, The associations between labor and delivery mode and maternal and placental oxidative stress, *Reprod. Toxicol.* 31 (2011) 144–150.